Available online at www.sciencedirect.com
SCIENCE DIRECT
Journal of Colloid and Interface Science 296 (2006) 165–177
JOURNAL OF Colloid and Interface Science
www.elsevier.com/locate/jcis

Synthesis and characterization of an electroactive surface that releases γ-aminobutyric acid (GABA)

Chun Yan [a,*,1], Wakana Matsuda [b,1], David R. Pepperberg [c], Steven C. Zimmerman [b,*], Deborah E. Leckband [a,b]

[a] *Department of Chemical and Biomolecular Engineering, University of Illinois at Urbana-Champaign, 600 S. Mathews Ave., Urbana, IL 61801, USA*
[b] *Department of Chemistry, University of Illinois at Urbana-Champaign, 600 S. Mathews Ave., Urbana, IL 61801, USA*
[c] *Department of Ophthalmology and Visual Sciences, University of Illinois at Chicago, 1855 W. Taylor Street, Chicago, IL 60612, USA*

Received 21 May 2005; accepted 16 August 2005

Available online 15 September 2005

Abstract

We report the synthesis and characterization of a new electroactive surface capable of releasing the neurotransmitter γ-aminobutyric acid (GABA) upon reduction. The GABA was anchored to an alkanethiol via electrochemically active quinone (abbreviation, TM-GABA). The quinone unit, upon reduction to the hydroquinone, cyclizes to release GABA into solution. The half-life is 99 s. The self-assembled monolayer (SAM) of TM-GABA on gold was prepared and characterized with several surface sensitive techniques. X-ray photoelectron spectroscopy (XPS) explored the SAM formation of TM-GABA on Au surfaces. Cyclic voltammograms showed the ability to electrochemically control the quinone unit at the distal end of the chain. GABA was selectively released upon electrochemical reduction at a potential of −700 mV. The functional GABA terminal group was detected by surface plasmon resonance measurements of anti-GABA antibody binding.

Keywords: Self-assembled monolayers (SAMs); XPS; SPR; Cyclic voltammogram; Electrochemical reduction; GABA

1. Introduction

Advances in the science and engineering of bioactive surfaces, as well as the broader areas of micro- and nanofabrication, make possible the design and assembly of ligand-modified surfaces with chemically defined composition and structure, and with bioactivity toward specific ligands and physiologically active tissues [1–6]. One challenging and exciting possible application of such bioactive surfaces is their use as a prosthetic device at chemical synapses in diseased neural tissue. For example, retinal degenerative diseases such as age-related macular degeneration (AMD) and retinitis pigmentosa (RP) involve the deterioration of rod and cone photoreceptors but are thought in certain cases to preserve the functionality of post-photoreceptor retinal neurons [7–9]. In such cases, an implantable device that, in response to an external signal (e.g., light), presented neurotransmitter to post-synaptic membrane receptors of remaining healthy neurons could restore stimulus-dependent function of the diseased tissue (e.g., in AMD and RP, light-dependent activity of post-photoreceptor retinal neurons) [10,11]. The present study was undertaken to develop a prototype surface preparation capable of releasing free neurotransmitter in response to an electrical signal. As the test neurotransmitter to be incorporated in this preparation, we chose γ-aminobutyric acid (GABA), the native neurotransmitter of multiple classes of chemical synapses found in retina and other tissues of the central nervous system.

The release of neurotransmitters from a surface at an appropriate moment in response to an electrical signal is becoming an important objective, considering its applications [12–15]. However the strategy for designing a well-controlled interface that releases neurotransmitter instantly has not yet been well-documented. Previous studies have suggested the use of specific

* Corresponding authors. Faxes: +1 217 333 5052, +1 217 244 9919.
E-mail addresses: cyan@uiuc.edu (C. Yan), sczimmer@uiuc.edu (S.C. Zimmerman).
[1] These authors contributed equally to the work. W. Matsuda conducted all syntheses and C. Yan carried out all surface analyses.

0021-9797/$ – see front matter
doi:10.1016/j.jcis.2005.08.029

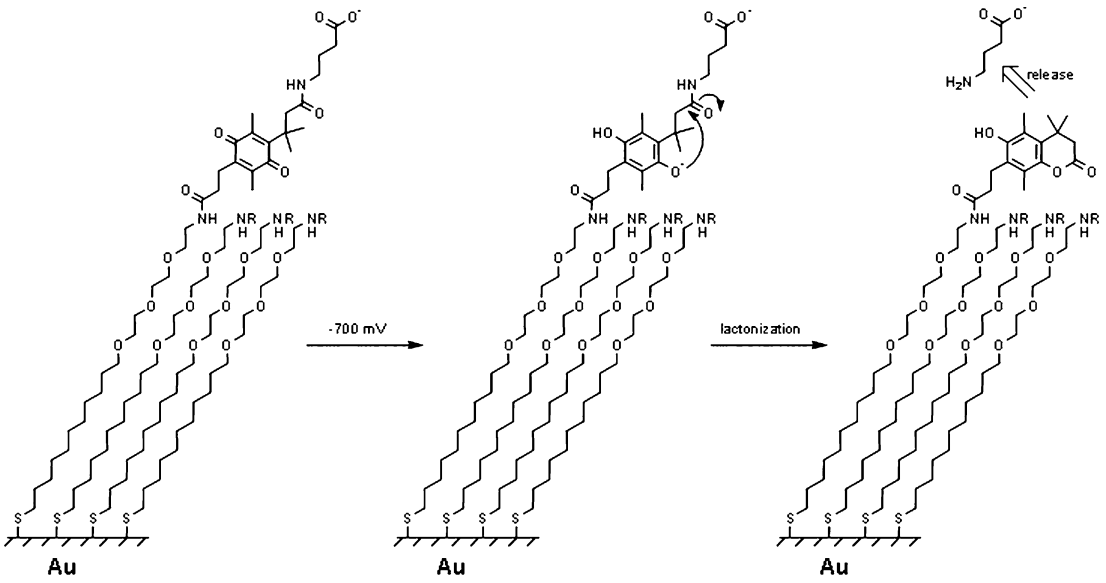

Fig. 1. Electrochemical reduction of a self-assembled TM-GABA monolayer on gold. The alkanethiol linked to gold surface organizes the TM-GABA into a close packed self-assembled monolayer structure while the triethylene glycol units provide a hydrophilic layer near the aqueous surface. The electroactive quinone unit releases GABA upon reduction. The overall design follows that pioneered by Mrksich and co-workers (see text).

design elements. For example, Mrksich and colleagues [1,3–5] tethered various electroactive units to gold via chains containing both a polymethylene segment and a PEO (polyethylene oxide) segment to achieve electrochemical control of redox reactions at the chain's distal end. The polymethylene segments of the attached chains collectively form a well-defined SAM structure near the gold surface [16–18], whereas the PEO units create a hydrophilic layer in contact with the aqueous solution. The latter was shown to inhibit protein absorption [19].

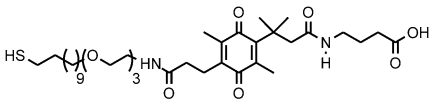

1

Our approach for transducing an electrical signal into the release of the neurotransmitter GABA is shown in Fig. 1. The actual compound studied, **1**, borrows from a biotin releasing surface recently reported by Hodneland and Mrksich [5], which in turn, built upon the earlier protecting group chemistry and the pro-drug approach developed by Carpino, Wang, and Borchardt [20–22]. Herein we describe the synthesis of **1** and the preparation of self-assembled monolayers (SAMs) of this material on gold surfaces. The molecular composition, electrochemical behavior, and the biological activity of the SAM were characterized by XPS, SPR and cyclic voltammetry. The aggregate evidence supports the electrochemically stimulated release of GABA. We also tested monolayers comprising a mixture of TM-GABA (**1**) and an oligo(ethylene glycol) (OEG)-terminated alkanethiol on gold in order to achieve additional control of the chain packing density. To our knowledge, this is the first report of the synthesis of TM-GABA (**1**) and the characterization of TM-GABA monolayers using different surface-sensitive techniques.

2. Experimental

2.1. General

Reagents and solvents used in reactions were obtained from commercial sources and were used without further purification except as follows: tetrahydrofuran (THF) was distilled from sodium benzophenone ketyl. *N*,*N*-dimethylformamide (DMF) was dried over 4 Å molecular sieves. Methylene chloride (CH_2Cl_2) and triethylamine were distilled from CaH_2. All reactions were monitored by TLC using silica gel 60 F_{254} glass plates (Merck). Flash chromatography was performed with 32–63 μm silica gel (Merck).

^{1}H NMR and ^{13}C NMR data were obtained on either 400 or 500 MHz Varian U400 and U500 instruments in chloroform-*d* ($CDCl_3$) unless otherwise noted. ^{1}H NMR spectra obtained in $CDCl_3$ were referenced to 7.26 ppm, and those obtained in D_2O were referenced to 4.79 ppm. ^{13}C NMR spectra obtained in $CDCl_3$ or D_2O were referenced to 77.00 ppm. Chemical shifts are reported in parts per million (ppm) and coupling constants are reported in hertz (Hz). IR spectra were collected on a Mattson FTIR 5000 with major bands reported in cm^{-1}. UV/vis spectra were obtained using a Shimadzu UV-2501PC recording spectrophotometer. FAB-MS and EI-MS data were collected by the mass spectrometry service at the University of Illinois at Urbana-Champaign (UIUC). Elemental analysis was performed in the microanalytical laboratory at UIUC.

The mixed triethylene glycol alkanethiol, $HO(CH_2CH_2O)_6(CH_2)_{11}SH$ (EG6) was custom synthesized by Obiter Research, LLC, Urbana, USA. Rabbit IgG (purified immunoglobulin reagent grade) and monoclonal anti-γ-aminobutyric acid (clone GB-69, abbreviation: anti-GABA) were purchased from Sigma, St. Louis, MO. GABA-OBu^t [23], 2-[2-(2-undec-10-enyloxyethoxy)ethoxy]ethanamine **8** [24], **3** [22], and **7** [20–22] were prepared according to known methods.

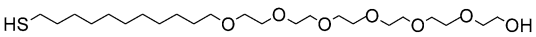

EG6

2.2. Kinetic measurements

Kinetic measurements generally followed the method reported by Amsberry and Borchardt [25]. A buffer solution was prepared with 0.050 M $NaH_2PO_4{\cdot}H_2O$ using water doubly distilled and deionized using a Corning Mega-Pure system MP-1. The pH was adjusted to 7.2 by adding HCl. pH measurements were made with an Orion Model 611 digital ion analyzer. The reactions were conducted at a temperature of 37.3 °C in an oil bath using an IKA Labortechnik mechanical stirrer ETS-D4 system.

A 10^{-3} M stock solution of quinone **2** was prepared by dissolving 0.30 mg (0.73 μmol) of **2** in 0.73 ml of HPLC grade CH_3CN. 200 μl of this solution were combined with 20 μl of a 0.1 M solution of $NaBH_4$ in the buffer solution described above at 37.3 °C. Quinone **2** was immediately reduced to its hydroquinone form (**4**). The resultant solution was diluted with 2 ml of buffer solution to give a final concentration of 1×10^{-4} M. Aliquots were removed from the reaction mixture at various times and frozen in a liquid nitrogen bath, stopping the reaction instantaneously. The samples were stored in a freezer before analyzing them by the HPLC assay described below.

2.3. HPLC assay conditions

The appearance of lactone **6** in the samples was monitored through the use of a Varian HPLC system consisting of a SD-200 pump and UV-1 UV detector. The analytical assay was conducted with a 1.0 ml/min flow rate on an ODS Hypersil C-18 column (5 μm, 150 × 4.6 mm). The eluting solution was a 50% (v/v) CH_3CN-aqueous solution adjusted to pH 3.2 with 0.01 M phosphate buffer. The lactone was quantified by measuring peak areas at $\lambda_{max} = 250$ nm.

2.4. Antibody solutions

Antibody solutions were prepared with a buffer containing 20 mM HEPES (Enzyme grade, Fisher Scientific, USA) and 150 mM sodium chloride (Fisher Scientific, USA), at pH 7.70. The protein solutions were prepared by adding the powder to the buffer to reach a final concentration of 0.1 mg/ml.

2.5. Substrate preparation

To prepare the gold films on glass slides, microscope slides were first cleaned with a 1:1:1 solution of $HCl/H_2O_2/H_2O$ at 65 °C for 40 min, rinsed thoroughly with purified water, and dried under a stream of nitrogen. A 20-Å chromium adhesion layer was thermally evaporated onto the slides at a rate of 0.1 Å s^{-1}, and the 400-Å Au layer was subsequently deposited at a rate of 1.0 Å s^{-1}. Self-assembled monolayers (SAMs) of pure TM-GABA were prepared by immersing the gold-coated glass slides in a 0.1 mM ethanolic solution of TM-GABA at room temperature. The mixed monolayers were adsorbed onto gold from two-component thiol solutions containing TM-GABA and EG6 molecules at different molar ratios. After 24 h, the samples were rinsed extensively with absolute ethanol, and blown dry with filtered nitrogen gas.

2.6. X-ray photoelectron spectroscopy (XPS)

XP spectra were recorded with a Physical Electronics PHI 5400 X-ray photoelectron spectrometer equipped with dual Mg$K\alpha$ ($h\nu = 1253.6$ eV) and Al$K\alpha$ ($h\nu = 1486.6$ eV) sources, typically operated at 300 W. Spectra were taken with Mg$K\alpha$ anode at a pass energy of 36 eV. The pressure in the analyzing chamber during the measurements was less than 9×10^{-9} Torr. The energy scale was referenced to the Au4$f_{7/2}$ resonance at the binding energy of 84.0 eV. The fitting of the spectra was done by a nonlinear least-squares procedure using simple Gaussian line shapes [26]. Prior to peak fitting, a background subtraction was performed by the Shirley method [27].

2.7. Cyclic voltammetry

Cyclic voltammetry was carried out with a Cypress Systems Microprocessor controlled OMNI-101 Analog Potentiostat (Cypress Systems, Inc., Lawrence, KS). Cyclic voltammograms (CVs) were collected with the in situ electrochemical SPR flow cell. The CVs were run between 0 and −1500 mV in a strong electrolyte of 0.25 M KOH/H_2O and in a neutral Ringer solution with a sweep rate of 50 mV s^{-1}. Ringer solution with a pH of 7.45 contained 100 mM NaCl, 2 mM KCl, 2 mM $CaCl_2$, 1 mM $MgCl_2$, and 5 mM HEPES.

2.8. Surface plasmon resonance (SPR) measurements

The surface plasmon resonance (SPR)-electrochemical experiments were performed with a home-built fluid flow cell designed for combined in situ SPR and electrochemistry measurements (see Fig. 2). The cell has an inlet port and an outlet port. The cell volume is ∼1.5 ml. The active area of the electrode (defined by a rubber O-ring) is 0.79 cm^2. A three-electrode

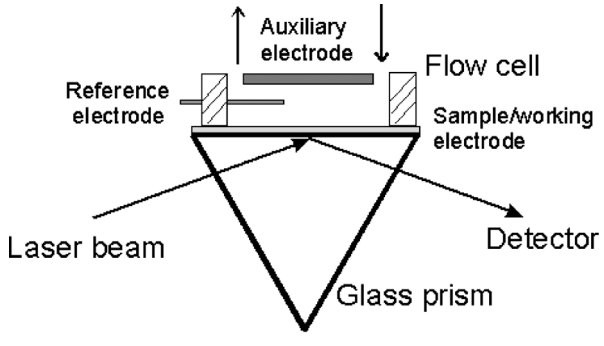

Fig. 2. A schematic diagram of the surface plasmon resonance sensor combined with the three electrode system for simultaneous electrochemical and molecular adsorption studies. The glass substrate is covered with thin gold film, modified with a self-assembled monolayer. This serves as the working electrode. A stainless steel plate is used as the auxiliary electrode, and the saturated Ag/AgCl is the reference electrode. The flow cell is used to adsorb protein from the solution flowing over the sample, as indicated by the arrows.

system was used. This consisted of a saturated Ag/AgCl as a reference electrode, a SAM/gold working electrode, and a stainless steel plate (10 mm diameter) auxiliary electrode. The solutions entering the cell were deaerated by purging with argon gas for at least 30 min. Another flow cell was also used to perform electrochemical reduction for different sample sizes. All of the electrochemical measurements were carried out at room temperature. The surface coverage of electro-active species was measured by integrating the reductive stripping peaks in the voltammograms, assuming a two-electron reduction process.

SPR measurements were performed with a custom-built, computer controlled apparatus based on the Kretchman configuration [28]. Briefly, the instrument consists of a precision goniometer (Oriel) driven by a stepper motor, an equilateral triangle prism, a large area Si-photodiode, and a GaAs laser (5 mW, 665 nm) light source. The electrochemical flow cell was also used to quantify the antibody adsorption to the TM-GABA monolayer. A system of three-way valves was used to inject the sample or to change the solutions without introducing air bubbles into the cell. The SPR cell containing the samples was first flushed with deionized water, followed by the buffer solution. Binding was initiated by injecting antibody solution at a flow rate of 0.1 ml/min into the flow cell. After the substrates were saturated with protein, the cell was flushed with the buffer solution. This procedure was repeated several times in order to remove non-specifically adsorbed antibody from the gold surface. The resulting change in the plasmon resonance angle corresponded to the amount of the bound antibody [1–5, 28,29]. All data were recorded at room temperature.

2.9. Chemical syntheses

2.9.1. Compound **2**

To a solution of 111.4 mg (0.47 mmol) of **3** and 171.6 mg (0.47 mmol) of TsOH·GABA-OBn in 10 ml of CH_2Cl_2 were added at 0 °C under a nitrogen atmosphere in sequence: 63.5 mg (0.47 mmol) of HOBt, 66 µl (0.47 mmol) of triethylamine, 97.0 mg (0.47 mmol) of DCC, and 11.5 mg (0.094 mmol) of DMAP. The mixture was stirred at 0 °C for 1 h and at room temperature for another 12 h. The reaction mixture was cooled in an ice-bath and the white precipitate (dicyclohexylurea, DCU) was filtered off. The filtrate was washed with 10 ml of a saturated aqueous solution of $NaHCO_3$, 10 ml of a 5% (w/v) aqueous solution of citric acid, and 10 ml of water. The organic layer was dried over $MgSO_4$, filtered, and evaporated. The residue was purified by flash chromatography (19:1 $CHCl_3$–EtOAc) to afford 40.4 mg (21%) of **2** as yellow oil: ^{1}H NMR δ 7.38–7.31 (m, 5H), 6.40 (q, $J = 1.5$ Hz, 1H), 5.66 (br s, 1H), 5.11 (s, 2H), 3.19 (q, $J = 7.0$ Hz, 2H), 2.76 (s, 2H), 2.36 (t, $J = 7.0$ Hz, 2H), 2.09 (s, 3H), 2.00 (d, $J = 1.5$ Hz, 3H), 1.78 (pentet, $J = 7.0$ Hz, 2H), 1.40 (s, 6H); ^{13}C NMR δ 191.2, 187.3, 173.2, 171.9, 154.1, 149.0, 137.4, 135.7, 130.9, 128.6, 128.4, 128.2, 66.4, 49.0, 38.7, 38.3, 31.6, 28.6, 24.4, 15.9, 13.8; FAB-MS m/z: 412.2 (M + H$^+$); HRMS–FAB m/z (M + H$^+$) calcd for $C_{24}H_{30}NO_5$, 412.2124; found, 412.2126. Anal. calcd for $C_{24}H_{29}NO_5 \cdot H_2O$: C, 67.11; H, 7.27; N, 3.26. Found: C, 67.02; H, 7.07; N, 3.56.

2.9.2. Compound **9**

A solution of 394 mg (1.17 mmol) of compound **7** and 158 mg (1.17 mmol) of HOBt were dissolved in 10 ml of CH_2Cl_2. The solution was cooled to 0 °C and 309.5 mg (1.17 mmol) of DCC was added and the mixture stirred for 30 min. A solution of 78.9 mg (0.78 mmol) of triethylamine and 235.9 mg (0.78 mmol) of **8** in 10 ml of CH_2Cl_2 was added followed by 28.1 mg (0.23 mmol) of 4-(dimethylamino)pyridine (DMAP). The solution was stirred at room temperature overnight. The reaction solution was cooled in an ice-bath, and the white precipitate, DCU, was filtered off. After evaporation, the residue was dissolved in 5 ml of ethyl acetate to precipitate the DCU, which was filtered off. The filtrate was washed with 5 ml of a 5% (w/v) aqueous solution of citric acid, dried over $MgSO_4$, and evaporated to give yellow oil. The crude oil was purified by column chromatography on silica gel (ethyl acetate) to afford 467.5 mg (97%) of the product **9** as a colorless oil: ^{1}H NMR δ 6.16 (t, $J = 5.2$ Hz, 1H), 5.79 (ddt, $J = 17.0$, 10.4, 6.8 Hz, 1H), 5.00–4.90 (m, 2H), 4.90 (s, 2H), 3.62 (s, 2H), 3.63–3.54 (m, 10H), 3.47–3.45 (q, $J = 5.2$ Hz, 2H), 3.41 (t, $J = 6.8$ Hz, 2H), 3.03–2.97 (m, 2H), 2.54 (s, 2H), 2.38–2.35 (m, 2H), 2.35 (s, 3H), 2.24 (s, 3H), 2.02 (q, $J = 6.8$ Hz, 2H), 1.57–1.52 (m, 2H), 1.43 (s, 6H), 1.37–1.31 (m, 2H), 1.25 (br s, 10H); ^{13}C NMR δ 172.3, 168.3, 151.8, 146.3, 139.2, 132.8, 129.1, 126.5, 123.7, 114.1, 100.0, 71.5, 70.52, 70.46, 70.2, 70.0, 69.8, 57.6, 45.7, 39.2, 36.0, 35.6, 33.7, 29.51, 29.47, 29.38, 29.36, 29.0, 28.8, 27.4, 26.0, 23.6, 15.7, 12.2; UV (MeOH) $\lambda_{max}(\varepsilon)$ nm 317 (324), 285 (1641), 278 (1590), 206 (43557); IR (neat) 1770, 1655 cm^{-1}; FAB-MS m/z 620.4 (M + H$^+$). Anal. calcd for $C_{35}H_{57}NO_8 \cdot 0.5H_2O$: C, 66.85; H, 9.30; N, 2.23. Found: C, 66.73; H, 9.19; N, 2.61.

2.9.3. Compound **10**

To a solution of 1.17 g (1.89 mmol) of **9** in 23 ml of THF were added 338 µl (4.73 mmol) of thiolacetic acid and 31 mg (190 µmol) of 2,2′-azobisisobutyronitrile (AIBN). Nitrogen gas was bubbled through the solution for 15 min. The mixture solution was irradiated in a photochemical reactor (Rayonet reactor lamp, 350 nm) for 18.5 h under an argon atmosphere. The loss of an allyl group peak was monitored by ^{1}H NMR. The solution was evaporated and the residue was purified by column chromatography on silica gel (ethyl acetate) to afford 1.08 g (82%) of **10** as a colorless oil, which slowly turned to a white solid: ^{1}H NMR δ 6.24 (t, $J = 5.2$ Hz, 1H), 4.89 (s, 2H), 3.61 (s, 2H), 3.62–3.53 (m, 10H), 3.44 (q, $J = 5.2$ Hz, 2H), 3.40 (t, $J = 6.8$ Hz, 2H), 3.01–2.99 (m, 2H), 2.83 (t, $J = 7.3$ Hz, 2H), 2.53 (s, 2H), 2.38–2.33 (m, 2H), 2.34 (s, 3H), 2.30 (s, 3H), 2.23 (s, 3H), 1.54–1.50 (m, 4H), 1.42 (s, 6H), 1.33–1.29 (m, 2H), 1.23 (br s, 12H); ^{13}C NMR δ 196.1, 172.2, 168.2, 151.7, 146.2, 132.8, 129.1, 126.5, 123.6, 100.0, 71.5, 70.5, 70.4, 70.2, 69.93, 69.85, 57.6, 45.7, 39.1, 36.0, 35.5, 30.6, 29.48, 29.45, 29.40, 29.35, 29.04, 29.01, 28.7, 27.3, 25.6, 23.6, 15.7, 12.2; UV (MeOH) $\lambda_{max}(\varepsilon)$ nm 285 (2114), 278 (2087); IR (neat) 1770, 1691 cm^{-1}; FAB-MS m/z 696.5 (M + H$^+$). Anal. calcd for $C_{37}H_{61}NO_9S$: C, 63.85; H, 8.83; N, 2.01. Found: C, 63.83; H, 8.97; N, 2.21.

*2.9.4. Compound **11***

A solution of 939 mg (1.35 mmol) of the compound **10** in a mixture of 27 ml (13.5 mmol) of a 0.5 N aqueous solution of HCl and 70 ml of a 1:1 (v/v) solution of MeOH–THF was stirred at room temperature for 2 days. The solvents were removed at reduced pressure and the residue was dissolved in 30 ml of ethyl acetate, washed with water (3 × 10 ml), and dried over $MgSO_4$. Filtration and evaporation gave 841 mg (96%) of **11** as a colorless oil: ^{1}H NMR δ 9.40 (s, 1H), 6.63 (br t, 1H), 3.62–3.50 (m, 10H), 3.45–3.40 (m, 4H), 2.95–2.93 (m, 2H), 2.85 (t, $J = 7.4$ Hz, 2H), 2.65–2.63 (m, 2H), 2.53 (s, 2H), 2.38 (s, 3H), 2.32 (s, 3H), 2.19 (s, 3H), 1.55 (m, 4H), 1.43 (s, 6H), 1.35–1.25 (m, 14H); ^{13}C NMR δ 196.2, 174.4, 169.0, 150.3, 143.2, 129.2, 126.1, 122.42, 122.40, 71.54, 70.48, 70.45, 70.2, 70.0, 69.4, 46.1, 39.8, 35.5, 34.9, 30.6, 30.3, 29.52, 29.46, 29.4, 29.11, 29.06, 28.8, 27.6, 27.5, 26.0, 21.1, 14.8, 12.1; UV (MeOH) $\lambda_{max}(\varepsilon)$ nm 289 (3341); IR (neat) 1765, 1691, 1645 cm^{-1}; FAB-MS m/z 652.3 (M + H$^+$). Anal. calcd for $C_{35}H_{57}NO_8S$: C, 64.48; H, 8.81; N, 2.15. Found: C, 64.48; H, 8.63; N, 2.22.

*2.9.5. Compound **12***

To a solution of 96.7 mg of **11** (148 μmol) in 14 ml of acetonitrile was added dropwise a solution of 31.7 mg of NBS (178 μmol) in 14 ml of water with stirring at room temperature. The solution turned to yellow immediately and was stirred for 10 min. The solution was extracted 2 times with 5 ml of ether, and the combined ether layers washed 2 times with 5 ml of water, and dried over $MgSO_4$. Filtration and removal of solvent at reduced pressure gave 96.4 mg (98%) of the crude quinone-propionic acid as yellow oil: ^{1}H NMR δ 6.32 (br t, 1H), 3.62 (s, 4H), 3.44 (t, $J = 7.0$ Hz, 2H), 3.35 (q, $J = 5.0$ Hz, 2H), 2.87–2.84 (m, 2H), 2.86 (s, 2H), 2.82 (t, $J = 6.0$ Hz, 2H), 2.32 (s, 3H), 2.27 (t, 2H, $J = 6.0$ Hz, 2H), 2.12 (s, 3H), 1.96 (s, 3H), 1.56 (m, 4H), 1.46 (s, 6H), 1.36–1.26 (m, 14H). The quinone prepared above (0.144 mmol) was dissolved in 5 ml of dry CH_2Cl_2 and a solution of 91.9 mg (173 μmol) of benzotriazoloy-tris[pyrrolidino]phosphonium hexafluorophosphate (PyBOP), 45.8 mg (288 μmol) of GABA-OBu^t in 1 ml of CH_2Cl_2 was added followed by 30.1 μl (173 μmol) of DIEA. The mixture was stirred at room temperature for 14 h under a nitrogen atmosphere. The solvent and volatile reagents were removed under reduced pressure and the residue was dissolved in 30 ml of CH_2Cl_2, washed with water (3 × 10 ml), and dried over $MgSO_4$. Filtration, concentration under reduced pressure, and purification by column chromatography on silica gel (1:2 PE–ethyl acetate) afforded 76.5 mg (65% from **11**) of **12** as pale yellow oil: ^{1}H NMR δ 6.32 (br t, 1H), 5.70 (br t, 1H), 3.65–3.60 (m, 10H), 3.54 (t, $J = 5.2$ Hz, 2H), 3.46–3.41 (m, 2H), 3.18 (q, $J = 7.2$ Hz, 2H), 2.85 (t, $J = 7.2$ Hz, 2H), 2.77 (s, 2H), 2.75–2.71 (m, 2H), 2.32 (s, 3H), 2.32–2.28 (m, 2H), 2.22 (t, $J = 7.2$ Hz, 2H), 2.10 (s, 3H), 2.02 (s, 3H), 1.71 (pentet, $J = 7.2$ Hz, 2H), 1.58–1.51 (m, 4H), 1.43 (s, 9H), 1.41 (s, 6H), 1.35–1.25 (m, 14H); ^{13}C NMR δ 196.1, 191.3, 172.9, 172.0, 171.8, 154.0, 145.0, 139.8, 137.3, 80.6, 71.5, 70.51, 70.45, 70.2, 69.98, 69.97, 49.0, 39.2, 38.8, 38.1, 35.1, 32.9, 29.52, 29.50, 29.44, 29.43, 29.40, 29.10, 29.05, 28.8, 28.0, 26.0, 24.5, 23.1, 14.0, 12.5; UV (MeOH) $\lambda_{max}(\varepsilon)$ nm 413 (124), 328 (sh, 528), 263 (11429); IR (neat) 1728, 1691, 1643 cm^{-1}; FAB-MS m/z 809.6 (M + H$^+$). HRMS–FAB m/z (M + H$^+$) calcd for $C_{43}H_{73}N_2O_{10}S$, 809.4986; found, 809.7988. Anal. calcd for $C_{43}H_{72}N_2O_{10}S$: C, 63.83; H, 8.97; N, 3.46. Found: C, 63.41; H, 9.18; N, 3.60.

*2.9.6. Compound **13***

A solution of 41.7 mg (51.5 μmol) of compound **12** and 239.2 μl (3.11 mmol) of trifluoroacetic acid in 2 ml of CH_2Cl_2 was stirred at room temperature for 16 h. The solution was evaporated to give 74.4 mg of the acid as a pale brown oil. ^{1}H NMR δ 6.60 (br t, 1H), 3.64–3.40 (m, 14H), 3.23–3.18 (m, 2H), 2.86 (t, $J = 7.4$ Hz, 2H), 2.80 (s, 2H), 2.78–2.74 (m, 2H), 2.5–2.40 (m, 2H), 2.32 (s, 3H), 2.28–2.23 (m, 2H), 2.13 (s, 3H), 1.99 (s, 3H), 1.70–1.65 (m, 2H), 1.60–1.52 (m, 4H), 1.40–1.21 (m, 14H); FAB-MS m/z 753.5 (M + H$^+$). The residue was dissolved in 0.35 ml of a 6.4:1 (v/v) mixture of THF and 1,2-dimethoxyethane. The mixture was degassed using three freeze-thaw cycles and placed under a nitrogen atomosphere. A solution of 35.1 mg (0.0466 mmol) of $LiOH{\cdot}H_2O$ in 0.17 ml of water was added and the color turned from yellow to red. The mixture was stirred at room temperature for 1 h and cooled to 0 °C. A 1 N aqueous solution of HCl was added until acidic and the color turned to yellow. The solution was extracted with 3 times with 10 ml of CH_2Cl_2, the combined organic layers washed with 10 ml of brine, and dried over $MgSO_4$. Filtration, concentration, and column chromatography on silica gel ($CHCl_3$, then acetone) gave 25.8 mg (78%) of the **13** as colorless oil: ^{1}H NMR δ 6.72 (br t, 1H), 5.1 (br, 1H), 3.62–3.39 (m, 14H), 3.34–3.30 (m, 1H), 3.21–2.95 (m, 2H), 2.91–2.72 (m, 2H), 2.66 (t, $J = 7.4$ Hz, 2H), 2.40–2.30 (m, 5H), 2.11–2.00 (m, 2H), 2.09 (s, 3H), 1.65 (pentet, $J = 7.4$ Hz, 2H), 1.59–1.54 (m, 4H), 1.38–1.25 (m, 17H) 1.01, 0.79 (s, 6H); FAB-MS m/z 711.4 (M + H$^+$).

*2.9.7. Compound **14***

A solution of 140.1 mg (0.21 mmol) of the propanoic acid in 1 ml of a 6.4:1 (v/v) THF–1,2-dimethoxyethane mixture was degassed by three freeze-thaw cycles and placed under a nitrogen atmosphere. A solution of 88.2 mg (2.1 mmol) of $LiOH{\cdot}H_2O$ in 1.4 ml of water was added and the mixture was stirred at room temperature for 10 min. After cooling at 0 °C, a 2 N aqueous solution of HCl was added until acidic. The solution was extracted 2 times with 10 ml of CH_2Cl_2, and the combined organic layers washed with 5 ml of brine. The organic layers were dried over Na_2SO_4, filtered and evaporated to give a yellow oil. The residue was dissolved in 1 ml of DMF and 5 ml of CH_2Cl_2 and 28.4 mg (0.21 mmol) of HOBt and 87.6 mg (0.231 mmol) of *O*-benzotriazol-1-yl-*N*,*N*,*N*′,*N*′-tetramethyluronium hexafluorophosphate (HBTU) was added. The solution was cooled at 0 °C and 66.9 mg (420 μmol) of GABA-OBu^t and 73 μl (420 μmol) of DIEA were added. The mixture solution was stirred at 0 °C for 2 h, warmed to room temperature and stirred overnight under a nitrogen atmosphere. After evaporation, the residue was dissolved in 10 ml of ethyl

acetate, washed 3 times with 5 ml of water and dried over Na_2SO_4. Filtration, concentration, and column chromatography on silica gel (ethyl acetate) afforded 25.1 mg (16%) of the product **14** as yellow oil: ^{1}H NMR δ 6.26 (br t, 1H), 5.75 (br t, 1H), 3.63–3.56 (m, 8H), 3.53 (t, $J = 5.0$ Hz, 2H), 3.44–3.40 (m, 4H), 3.15 (q, $J = 7.0$ Hz, 2H), 2.76 (s, 2H), 2.73–2.70 (m, 2H), 2.66 (t, $J = 7.5$ Hz, 2H), 2.30–2.27 (m, 2H), 2.20 (t, $J = 7.0$ Hz, 2H), 2.09 (s, 3H), 2.01 (s, 3H), 1.69 (pentet, $J = 7.0$ Hz, 2H), 1.64, 1.55 (m, 4H), 1.42 (s, 9H), 1.39 (s, 6H), 1.38–1.25 (m, 14H); ^{13}C NMR δ 191.3, 187.2, 172.8, 172.0, 171.8, 154.0, 145.0, 139.8, 137.3, 80.6, 71.5, 70.52, 70.46, 70.2, 70.0, 69.8, 49.0, 39.2, 39.1 38.8, 38.1, 35.1, 32.9, 29.54, 29.52, 29.47, 29.44, 29.42, 29.19, 29.15, 28.7, 28.5, 28.0, 26.0, 24.5, 23.0, 13.9, 12.5; UV (MeOH) $\lambda_{max}(\varepsilon)$ nm 262 (12700); IR (neat) 1728, 1643 cm^{-1}; FAB-MS m/z 767.5 (M + H$^+$). HRMS–FAB m/z (M + H$^+$) calcd for $C_{41}H_{71}N_2O_9S$, 767.4880; found, 767.4880.

2.9.8. Compound **1** (**TM-GABA**)

A solution of 24.1 mg (31.4 μmol) of compound **14**, 0.145 ml (1.88 mmol) of trifluoroacetic acid, and 10 μl (62.6 μmol) of triethylsilyl hydride in 1.2 ml of CH_2Cl_2 was stirred at room temperature for 2 h under a nitrogen atmosphere. The solution was evaporated and the residue dissolved in 2 ml of CH_2Cl_2. The solution was washed 2 times with 0.5 ml of water, dried over Na_2SO_4, and filtered. The organic layer was evaporated and the residue purified by chromatography on silica gel (4:1 (v/v) $CHCl_3$–MeOH) to afford 8.5 mg (38%) of **1** (**TM-GABA**) as yellow oil which slowly solidified: ^{1}H NMR (D_2O) δ 3.60 (br s, 6H), 3.54 (br, 4H), 3.40 (br, 2H), 3.33 (br, 2H), 3.05 (br, 2H), 2.75 (m, 2H), 2.68 (br, 2H), 2.59 (s, 2H), 2.33 (br, 2H), 2.14 (t, $J = 7.2$ Hz, 2H), 2.04 (s, 3H), 1.99 (s, 3H), 1.66 (pentet, $J = 7.2$ Hz, 2H), 1.60, 1.51 (br, 4H), 1.36 (s, 6H), 1.28 (br s, 14H); ^{13}C NMR δ 191.7, 187.2, 182.4, 174.5, 173.6, 155.0, 145.6, 139.5, 137.0, 71.2, 70.2, 70.0, 69.9, 69.2, 48.1, 39.3, 39.0, 38.0, 34.8, 34.6, 29.4, 29.84, 29.79, 29.6, 29.5, 29.3, 28.7, 28.1, 26.2, 25.7, 22.9, 13.8, 12.4; UV (MeOH) $\lambda_{max}(\varepsilon)$ nm 263 (11731); FAB-MS m/z 711.4 (M + H$^+$), 733.4 (M + Na$^+$). HRMS–FAB m/z (M + H$^+$) calcd for $C_{37}H_{63}N_2O_9S$, 711.4254; found, 711.4257.

3. Results

Before initiating the synthesis of **1**, a model study was undertaken to measure the approximate rate of GABA release in an analogous quinone unit. Thus, compound **2** was synthesized from **3** [25] as shown in Scheme 1. The benzyl ester was used so that a chromophore would be present, allowing for HPLC detection of the release of GABA-OBn and for ease of synthesis and purification. The kinetic method used is detailed in Section 2. In short, **2** was chemically reduced to **4** with sodium borohydride and the rate of formation of lactone **6** was monitored by HPLC. The release of GABA-OBn (**5**) was also detected by HPLC. Reduction of quinone **2** was too fast for its rate of formation to be measured, but the rate of the lactonization step could be determined. Thus, at pH 7.2 and 37 °C the rate constant for lactonization was determined to be $k_{obs} = (7.03 \pm 0.66) \times 10^{-3}$ s^{-1}. The

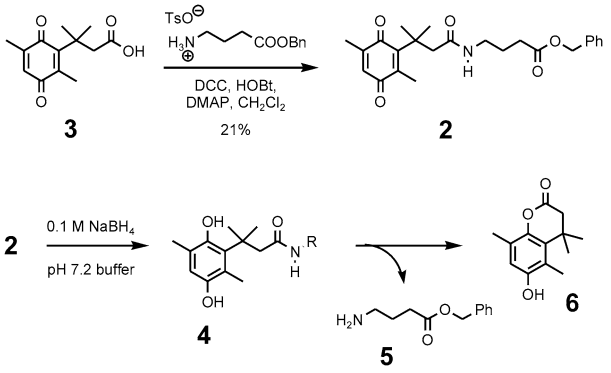

Scheme 1.

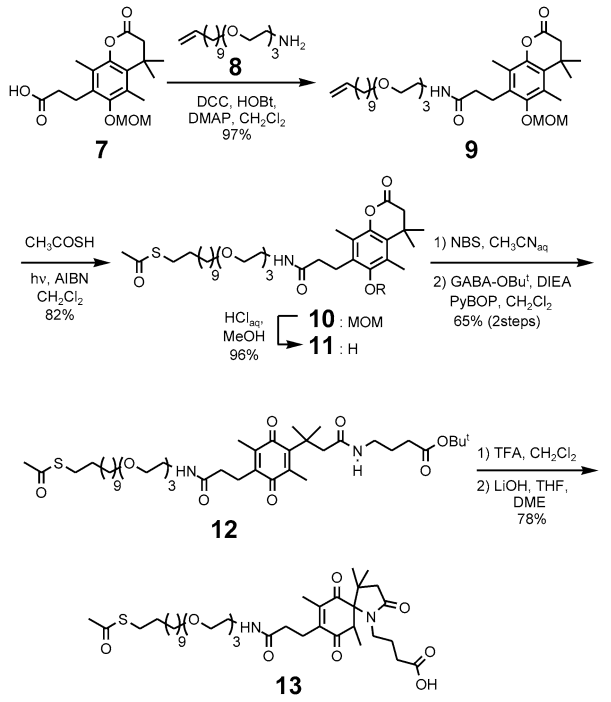

Scheme 2.

calculated half-life, $t_{1/2} = 99$ s, is approximately the same as measured by Amsberry and Borchardt for a structurally similar series of quinones [25].

The initial approach to the synthesis of **1** is outlined in Scheme 2. Carboxylic acid **7** was activated and treated with amine **8** to give amide **9** in high yield. Radical addition of thiolacetic acid to the terminal alkene afforded protected alkanethiol **10** in 82% yield. Removal of the MOM group with aqueous HCl produced **11** in high yield and subsequent NBS mediated oxidation to the quinone liberated the side-chain carboxylic acid group that was activated in situ and reacted with GABA-OBu^t to give **12**. The TFA mediated deprotection of the GABA amide occurred smoothly, but basic deprotection of the thiol acetate led to an undesired internal Michael addition and spirolactam **13**. The reaction has precedent in studies of a related quinone by Borchardt et al. [30]. Although not the desired product, **13** was regarded as a control compound and was used to compare with **1** (vide infra).

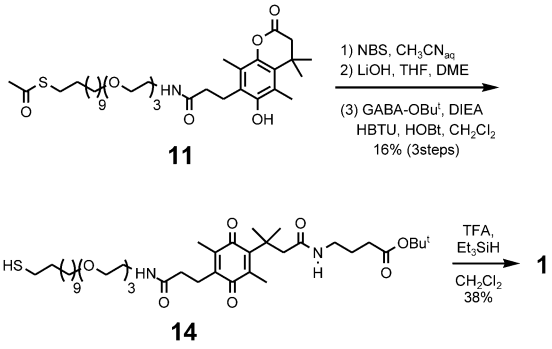

Scheme 3.

The successful synthesis of **1** (**TM-GABA**) is outlined in Scheme 3. Thus, lactone **11** was first oxidized to the quinone with NBS, then the thiol group liberated with LiOH, and, finally, activation of the propionic acid side-chain and reaction with GABA-OBu^t. The overall, unoptimized yield for the three steps was 16%. TFA-mediated removal of the *tert*-butyl ester group in the presence of triethylsilane gave **1** (**TM-GABA**) in 38% yield. The overall synthesis of TM-GABA from 2,5-dimethyl-1,4-benzophenone occurred in 16 steps and 1.3% yield.

Three types of self-assembled monolayers (SAMs) on gold were prepared. The first, illustrated in Fig. 1, was prepared from **1** and contained a dense layer of quinone for GABA release studies. The SAMs of the second type were used as references. These included one SAM prepared with EG6, a mixed alkane oligo(ethylene glycol) that was intended to mimic the tethering group in TM-GABA, and another SAM was prepared from spirolactam **13** (abbr. **TM-Spiro**). The third type was a two-component SAM derived from TM-GABA and EG6 mixtures. Several mixed SAMs were used to control surface density of TM-GABA.

3.1. Cyclic voltammetry

Fig. 3 shows the cyclic voltammograms of SAMs on gold surfaces in 0.25 M KOH and in Ringer solution. All of the monolayers have less double layer capacitance than the CVs measured on bare gold, confirming the monolayer formation on the gold surfaces. The negative current peak at −956 mV in the CV of the EG6 SAM (Fig. 3A) is due to the thiolate desorption. The peak intensities decreased with decreasing thiolate coverage, and shifted to positive potential (Fig. 3A). The reduction is presumed to be complete when the peak is no longer visible [31].

Three reductive reactions were observed with TM-GABA monolayers in 0.25 M KOH (Fig. 3B): namely two intense peaks at −629 and −966 mV, and one broad peak at about −1140 mV. The electrochemical reduction in Ringer solution (Fig. 3C) gave less pronounced and broad peaks at −570, −935, and −1160 mV, respectively. The peak assignments are not straightforward. For TM-Spiro on Au (Fig. 3D), there is one intense peak at −935 mV and a broad peak at ∼ −1140 mV in 0.25 M KOH. The TM-Spiro is a tautomer of TM-GABA. Therefore, the peaks at −629 mV in Fig. 3B and −570 mV in Fig. 3C are assigned, respectively to the quinone reduction, i.e., the cyclization reaction, and release of GABA. The peaks at −966 mV in Fig. 3B or −935 mV in Fig. 3C are tentatively assigned to the reduction of the TM-Spiro group, and the peak at −1140 mV (Fig. 3B) or −1160 mV (Fig. 3C) is attributed to the thiolate reduction. The calculated surface coverages of TM-GABA and EG6 on Au were, respectively, $(2.1 \pm 0.5) \times 10^{-10}$ and $(7 \pm 2) \times 10^{-10}$ mol cm^{-2}. The value for the EG6 SAM is in good agreement with a close-packed monolayer, which has a density of 7.7×10^{-10} mol cm^{-2} for a $(\sqrt{3} \times \sqrt{3})$ R30° overlay structure on Au(111) [31]. TM-GABA molecules form a less densely-packed film on Au, compared with EG6.

The co-adsorption of two or more thiols [32] enabled the adjustment of the TM-GABA surface density in the monolayer. Fig. 3E shows the cyclic voltammogram of a mixed monolayer in 0.25 M KOH. This mixed monolayer was formed from a 1:1 TM-GABA:EG6 solution. There are three reduction peaks, including one pronounced peak at −615 mV, and two broad peaks at −1035 and at −1220 mV. Fig. 3F shows the cyclic voltammogram of this mixed monolayer in Ringer solution. We similarly observed three broad reduction peaks at −600, −960, and −1160 mV. By comparing these data with the CVs of the pure TM-GABA monolayers, we assigned the peak at −615 mV (in KOH) or −600 mV (in Ringer solution) to the quinone reduction. The broad peak at ∼ −1000 mV was assigned to the combination of the thiolate reduction of the EG6 and to the reduction of the Spiro group. The peak at about −1200 mV is attributed to the reduction of the TM-GABA thiolate. The surface density of the thiols in this mixed monolayer was calculated by integrating the peaks at −615 or −600 mV, and −1035 or −960 mV, assuming a two-electron reduction process. The thus calculated TM-GABA density was $(1.2 \pm 0.1) \times 10^{-10}$ mol cm^{-2} and the EG6 density was $(3 \pm 0.1) \times 10^{-10}$ mol cm^{-2}. In order to increase the accessibility of the GABA molecule to anti-GABA antibody, the TM-GABA molecules were diluted in the mixed layers. The mixed monolayers formed from the solutions of 1:100 TM-GABA:EG6 were electrochemically reduced in 0.25 M KOH and in Ringer solution. No visible peak at ∼ −600 mV was seen in cyclic voltammograms, within the experimental error (data not shown).

3.2. XPS characterization

The surface composition and chemical states were characterized by XPS. Fig. 4 shows a series of XP spectra of pure EG6, TM-GABA and reduced TM-GABA SAMs. S2p XP spectra (not shown here), comprising a doublet corresponding to S2$p_{3/2}$ (binding energy of 162.1 eV) and S2$p_{1/2}$ peaks, were observed with these three monolayers, and are indicative of the Au–S thiolate bond [33]. The alkyl and ether carbon atoms in the as-formed EG6 SAM are distinguished by their distinct C1s peaks at binding energies of 284.8 and 286.6 eV, respectively (Fig. 4A) [34]. There was only one intense O1s peak, corresponding to the C–O bonds (Fig. 4B). In the XP spectra of the TM-GABA SAM, two peaks corresponding to O–C and O=C

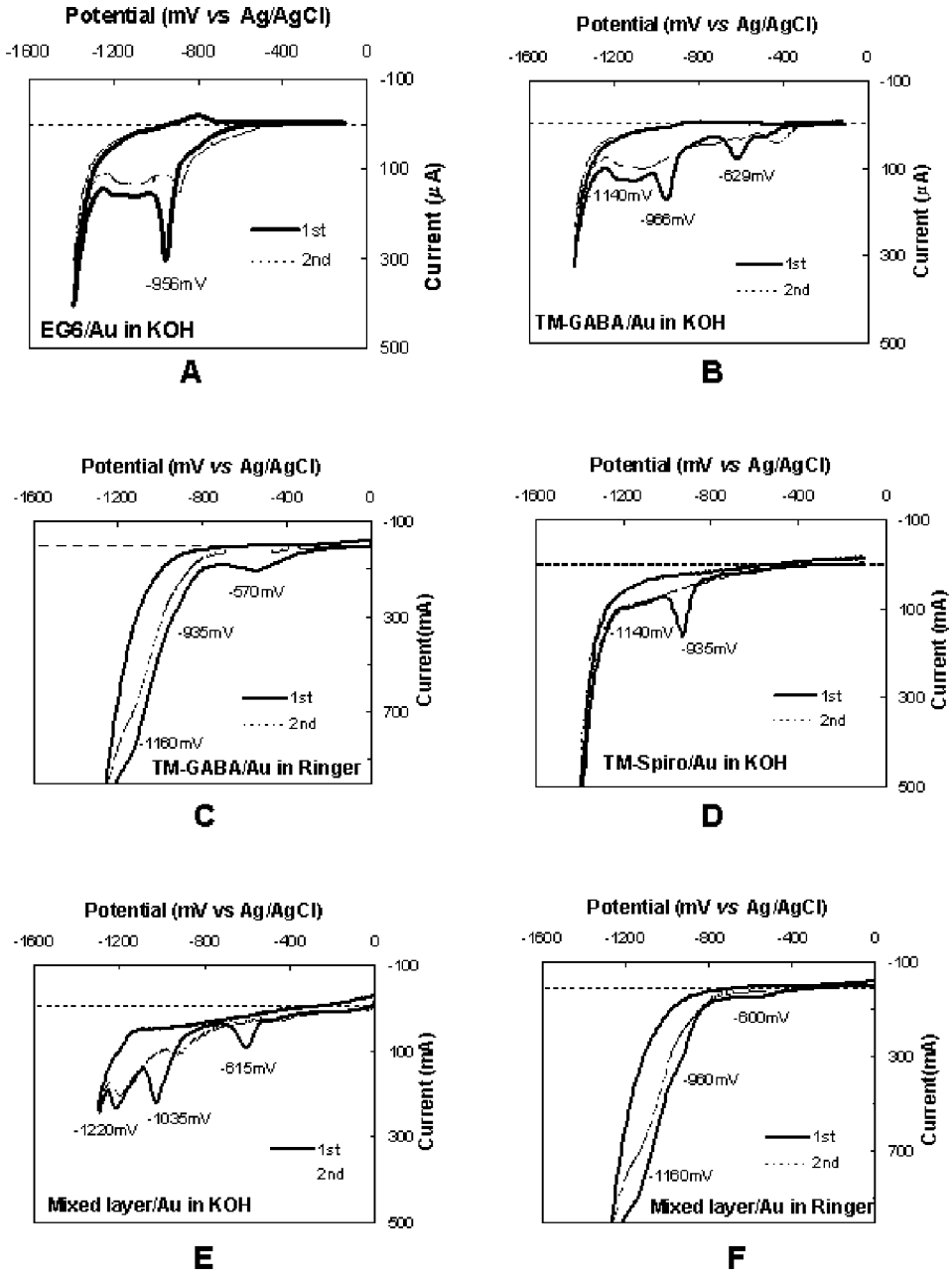

Fig. 3. Consecutive cyclic voltammograms of a monolayer of (A) EG6 and (B) TM-GABA, on gold surfaces in a solution of 0.25 M KOH/H_2O. (C) TM-GABA on gold surfaces in Ringer solution. (D) TM-Spiro and (E) mixed TM-GABA and EG6 SAMs in KOH/H_2O. (F) A mixed layer formed from 1:1 TM-GABA:EG6 mixture on gold surfaces in Ringer solution. The scan rate is 50 mV s^{-1} in each case. The solid curves represent the first reductive scan. The dashed lines represent the second scan.

were needed to fit the O1*s* peak (Fig. 4B). The C1*s* spectrum was fit with 3 peaks, corresponding to C–C, C–O, and C=O (Fig. 4A). Compared with the EG6 SAM (Fig. 4A), the C–C binding energy in the TM-GABA monolayer shows a distinct positive shift. This may be due to the greater influence of the headgroup electronegativity on the C–C binding energy in the long chain SAM, relative to the electron donating effect of the electropositive Au surface [35].

After the electrochemical reduction, the most significant change in the XP spectra of TM-GABA was the increased intensity from the Au substrate (spectra not shown), which indicated a decrease in film thickness.

The approximate thickness L of the monolayer was estimated from the attenuation of the Au4f signal, as described by the following equation [36],

$$L = \lambda \cos\theta \ln\left(\frac{I_{\mathrm{Au0}}}{I_{\mathrm{Au}L}}\right). \tag{1}$$

Here I_{Au0} is the Au4f intensity from a sputter cleaned Au surface; $I_{\mathrm{Au}L}$ is the intensity of Au photoelectrons attenuated by a homogeneous layer of thickness L; and θ describes the angle of the surface normal of the sample with respect to the analyzer axis. For our measurements $\theta = 45°$. A value of 37 Å [33] was

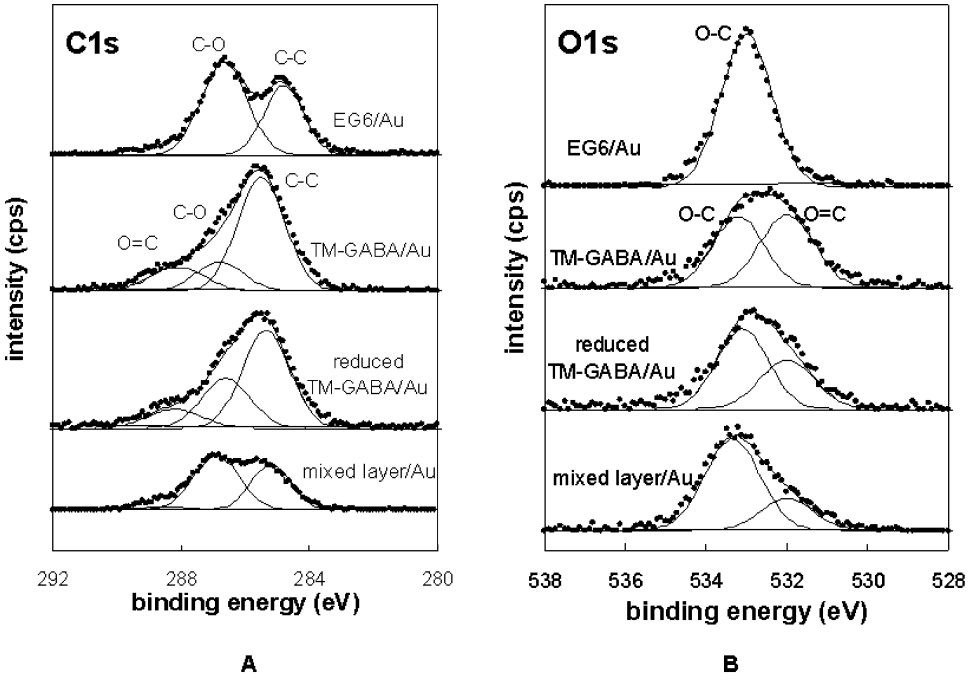

Fig. 4. X-ray photoelectron spectra of self-assembled monolayers of EG6, TM-GABA, reduced TM-GABA at −700 mV, and mixed SAMs generated from 1:1 TM-GABA:EG6 mixture. (A) C1*s* spectra and (B) O1*s* spectra of freshly prepared EG6, TM-GABA SAMs, electrochemically reduced TM-GABA at −700 mV, and mixed monolayers generated from 1:1 TM-GABA:EG6 mixture.

used for λ, the mean free path of photoelectrons through the layer.

The thus calculated monolayer thickness was 21 ± 1 Å and 39 ± 1 Å for the EG6 and TM-GABA monolayers, respectively. The EG6 thickness agrees with previous findings [34]. Considering the theoretical thickness of 45 Å for a fully extended chain, a layer thickness of 39 ± 1 Å for the TM-GABA SAM suggests a tilt angle of ∼30° with respect to the surface normal. After the electrochemical reduction of the TM-GABA monolayer at −700 mV, the layer thickness decreased to 29 ± 1 Å. This indicates a reduction of ∼10 Å in the layer thickness. This latter thickness difference roughly matches the length of the GABA group, and indicates the release of GABA upon electrochemical reduction. The TM-Spiro SAM had a thickness of only 26 Å, which suggests that the monolayer is less ordered.

Unlike the substrate Au intensity, the total intensities of carbon and oxygen signals did not change significantly after the electrochemical reduction. Fits of the XP spectra for C1*s* and O1*s* reveal quantitative changes in the O=C intensity, which decreased after the electrochemical reduction. Thus, another way to quantify GABA release following the electrochemical reduction is by calculating the ratio of C–O:C=O per unit area through the change of the peak intensities before and after the reduction. The calculated results were in accordance with a film structure in which the GABA is released. In order to assign the peak at −930 mV, we measured XP spectra of TM-GABA and TM-Spiro SAMs after a voltage sweep to −1000 mV. The spectra exhibit decreased intensities of the oxygen and carbon signals. For TM-GABA, the oxygen peak intensity decreased by $16 \pm 4\%$, and the carbon peak intensity decreased by $21 \pm 5\%$. The sulfur intensity increased slightly. These results suggest the reduction in the top, superficial region of the film. The thickness of the reduced monolayers was 19 ± 1 Å and 20 ± 1 Å for TM-GABA and TM-Spiro SAMs, respectively.

In the mixed monolayer, the XP nitrogen and C=O signals are convenient chemical markers for TM-GABA. The appearance of the N1*s* signal (spectrum not shown) and C=O confirmed the existence of TM-GABA in the mixed films. The C1*s* and O1*s* spectra in Fig. 4 also show a combination of TM-GABA and EG6 characteristics. The contribution of the TM-GABA is small, due to its low concentration. The shoulder on the O1*s* peak in the O=C region indicates that TM-GABA is present. Likewise, a shoulder on the main peak in the C=O region similarly confirms the presence of TM-GABA in the monolayer. Fits of the XPS spectra quantitatively confirmed the conclusions based on this visual inspection. It is important to point out that, during the fits, the FWHM (full width at half-maximum intensity) of individual peaks fitted in the O1*s* spectra was kept constant over the whole data set: 1.5 eV for O–C and 1.6 eV for O=C. From the measured changes in C1*s* and O1*s* spectra, the calculated ratio of TM-GABA:EG6 in the monolayers was ∼1:2, which is close to the value of 1:2.5 determined by cyclic voltammetry. The thickness of the mixed monolayer estimated from XP analysis and equation **1** is 23 ± 1 Å, which is surprisingly close to the thickness of EG6. This is inconsistent with the GABA extending out of the layer, and suggests that the latter may be bent over in the mixed film [37].

3.3. GABA accessibility in pure and mixed TM-GABA monolayers

Surface plasmon resonance measurements [38,39] were used to assess the accessibility of GABA to anti-GABA antibodies.

The control consisted of measurements of the non-specific adsorption of polyclonal IgG antibody to the TM-GABA SAMs and the non-specific adsorption of the monoclonal anti-GABA to the EG6 SAMs. Fig. 5A shows that no polyclonal IgG adsorbed on the TM-GABA monolayer. After applying a potential of −700 mV, the surface remained inert to polyclonal IgG adsorption. The pure EG6 monolayer was inert to both polyclonal IgG and monoclonal anti-GABA adsorption (data not shown), consistent with the reported protein resistance of pure EG6 monolayers [40–42].

By contrast, Fig. 5B shows that the monoclonal anti-GABA bound to both pure and mixed TM-GABA monolayers. With pure TM-GABA monolayers, the injection of the antibody solution resulted in a significant change in the plasmon resonance angle, which reflects the adsorption of the antibody (curve a). The anti-GABA was washed off gradually from the surfaces after flushing with buffer. Following the voltage sweep to −700 mV with the subsequent release of the GABA group in KOH/H_2O and in Ringer solution, the amount of anti-GABA adsorbed was reduced by 60% relative to the amount bound to the unreduced pure TM-GABA monolayer (curves b and c). With mixed monolayers generated from 1:1 TM-GABA:EG6 solution (curve d), the amount of antibody adsorbed was lower than obtained with the pure TM-GABA film. There is still about 33% antibody adsorption after electrochemical reduction (curve e). For the mixed monolayer generated from a 1:100 TM-GABA:EG6 solution (curve f), no anti-GABA antibody was detected within the experimental error.

4. Discussion

In TM-GABA (**1**), the two methyl groups at the benzylic position together with the proximal methyl group on the ring (referred to as a trimethyl lock), increase the rate of the lactonization [43]. The kinetic measurements revealed the instantaneous reduction of quinone to hydroquinone, as well as the rate of the lactonization step in solution. Analysis of the lactonization rate of compound **4** yielded a half-life time of 99 s for the release of GABA-OBn **5**. As this time scale of release, which is generally similar to that observed for other lactonizations [20,25], far exceeds the time scale of neural signaling at chemical synapses [44–46], further development of chemical and surface engineering strategies will be needed in order to achieve physiologically relevant device response times.

The self-assembled monolayer of TM-GABA (**1**) was prepared from its ethanolic solution. Although the TM-GABA chain is much longer than the EG6 molecule, both cyclic voltammetry and XPS experiments confirmed the formation of an ordered TM-GABA monolayer on gold after overnight immersion in ethanolic solution. The calculated thickness of the TM-GABA SAM is 39 ± 1 Å. Considering the theoretical thickness of 45 Å for a fully extended TM-GABA chain, this result suggests a tilt angle of ∼30° for TM-GABA monolayer with respect to the surface normal. TM-GABA SAMs also show a surface density close to the coverage expected for a $(\sqrt{3} \times \sqrt{3})$ R30° overlay structure on Au. Upon application of a reductive potential at −700 mV, the changes in the XP spectra indicated the release of GABA upon electrochemical reduction. The assignment of the reductive peak at around −630 mV in the cyclic voltammograms of TM-GABA SAMs to the quinone reduction, is consistent with previous results [5].

The assignment of the peak at −940 mV is more complex. Both the TM-GABA and TM-Spiro monolayers were reduced at −1000 mV. From the changes of main XP peak intensities, i.e., C1*s*, O1*s*, N1*s*, and S2*p*, the reduced film maintained the majority of the peak intensities, but the monolayer was thinned. The calculated thicknesses of the reduced monolayers were 19 ± 1 Å and 20 ± 1 Å for TM-GABA and TM-Spiro, respectively. Moreover, the peak at −940 mV was undetectable in the second CV scan of the TM-GABA monolayer. These data exclude the possibility of thiolate desorption at the reduction potential of −1000 mV. Instead, all of the data support a top layer reduction. The film thickness of ∼20 Å matches the length of the tethering group in the TM-GABA. The amide bonds are cleaved from the top quinone group, suggesting homolysis at −1000 mV. The broad peak appearing at −1140 mV is assigned to desorption of the thiolate monolayer.

The bio-specific binding of anti-GABA antibody to the GABA films, as verified by SPR, demonstrates the accessibility of GABA in these self-assembled films. This interaction decreased after an application of −700 mV to a pure TM-GABA SAM. The antibody coverage Γ (molec/cm^2) can be estimated from the measured SPR response [29] where

$$\Gamma\ (\text{molec cm}^{-2}) = d\ (\text{cm}) \times N\ (\text{molec cm}^{-3}).$$

The thickness of adsorbed antibody d (cm) was determined by SPR. The bulk number density of the antibody, N, was estimated from the bulk density of the crystalline protein. The anti-GABA antibody employed in the present experiments is a mouse IgG1 isotype. Based on the structure of IgG antibodies [47], a value of 7.27×10^{17} molec cm^{-3} for N was estimated for the bulk antibody density. Given the cross sectional area of anti-GABA [47], the maximum theoretical close-packed antibody coverage on these films would be 6.7×10^{11} molec cm^{-2}. The measured anti-GABA coverage on a full TM-GABA monolayer (Fig. 5B, curve a) was calculated from the SPR data to be 1.1×10^{11} molec cm^{-2}. The difference between the theoretical and experimentally measured values of antibody coverage is attributed to lateral steric repulsion between the antibodies and to the jamming limit, which limits coverage to ∼0.6 of a close packed monolayer.

The reduction in antibody binding following electrochemical reduction indicates substantial GABA conversion and release. The surface density of GABA groups on a full TM-GABA monolayer is $\sim(2.1 \pm 0.5) \times 10^{-10}$ mol cm^{-2} or $\sim 1.2 \times 10^{14}$ molec cm^{-2}. A close-packed antibody layer will therefore only occupy $[2 \times (6.7 \times 10^{11})/(1.2 \times 10^{14})] \times 100\% =$ 1.12% of the available sites, assuming bivalent antibody binding. Even a conversion of 98.9% would still leave 1.34×10^{12} GABA cm^{-2}, which would support the binding of a complete monolayer of antibody. For this reason, the amount of residual antibody binding cannot be used as a quantitative measure of TM-GABA conversion. It can, however, be used to

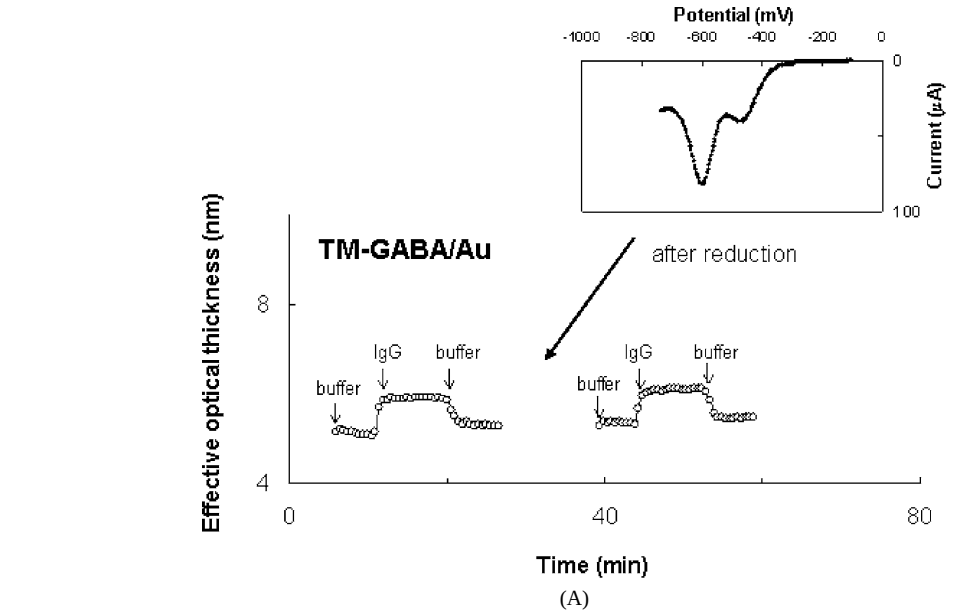

(A)

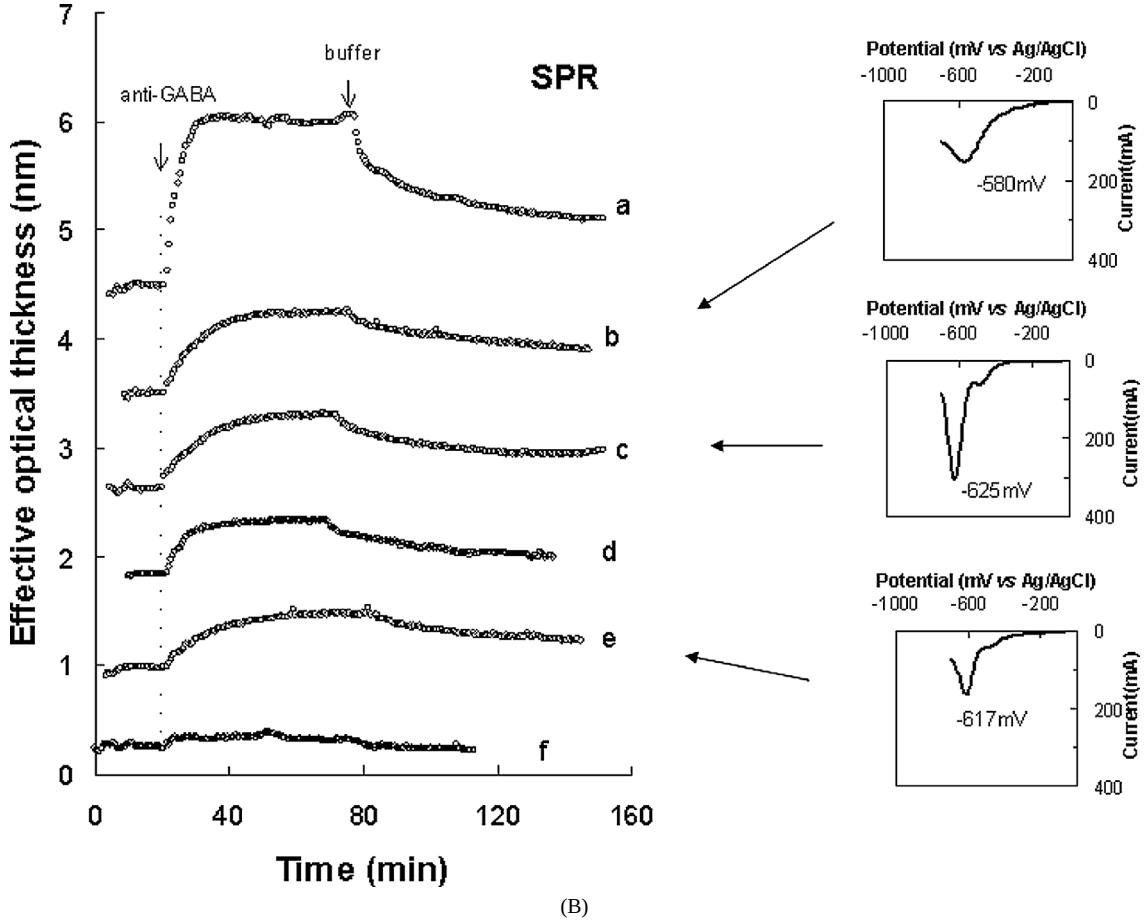

(B)

Fig. 5. Surface plasmon resonance measurements of antibody adsorption versus time on TM-GABA SAMs and the mixed TM-GABA:EG6 layers before and after electrochemical reduction. Vertical arrows indicate the time of solution injections. Antibody (IgG or anti-GABA) and buffer were injected as indicated. (A) SPR time course of the adsorption of polyclonal IgG on pure TM-GABA SAMs before (left) and after (right) electrochemical reduction. Insert (above right): first electrochemical reductive scan at a scan rate of 50 mV s^{-1}. (B) SPR time course of monoclonal anti-GABA antibody adsorption onto a pure TM-GABA SAM and on mixed TM-GABA:EG6 layers (left). The right-hand panels show the first electrochemical reductive scans with the corresponding monolayers before the SPR measurements were obtained. SPR curve (a) shows the adsorption of monoclonal antibody on the pure TM-GABA layer. Curve (b) shows the antibody adsorption on the TM-GABA SAM that was pre-reduced in Ringer solution at −700 mV. Curve (c) shows the adsorption on the TM-GABA SAM pre-reduced in KOH at −700 mV. Curve (d) shows the adsorption of anti-GABA antibody on the mixed SAM. The mixed layer was prepared from a 1:1 TM-GABA:EG6 mixture. Curve (e) indicates the adsorption of antibody on the mixed SAM that was pre-reduced in the KOH solution. The mixed layer was prepared from a 1:1 TM-GABA:EG6 mixture. Curve (f) indicates the anti-GABA adsorption on the mixed SAM prepared from 1:100 TM-GABA:EG6 mixture.

estimate an upper bound for the percentage of TM-GABA conversion. For example, following the reduction of the full TM-GABA monolayer (Fig. 5B, curves b and c), there was a 60% reduction in the amount of antibody retained on the surface. The amount of adsorbed antibody would be $0.4 \times (1.1 \times 10^{11}) = 4.4 \times 10^{10}$ antibodies cm^{-2}. If we assume 1:1 antibody:TM-GABA binding, then the amount of residual GABA on the surface would be 4.4×10^{10} GABA cm^{-2}. This is only $[(4.4 \times 10^{10})/(1.2 \times 10^{14})] \times 100\% = 0.04\%$ of the original GABA. If the antibody binding was bivalent, then the residual would still be 0.08%, which reflects a >99% conversion. Therefore, even a modest reduction of only 60% in antibody binding to the surface reflects a substantial loss of GABA. This conclusion is supported by the XPS and CV data. A previous report [5] assumed that 95% conversion reflected complete electrochemical release. The analysis of these antibody adsorption data in this study indicates that GABA release is at least as efficient.

Previous work used protein binding at lower ligand densities to assess the electrochemical conversion [5]. Here, we attempted a similar measurement with mixed TM-GABA and EG6. The cyclic voltammetry and XP results of the mixed films confirmed the formation of mixed monolayers. However, the determined thicknesses of the resultant films showed that the mixed film was thinner than the full TM-GABA film. The TM-GABA does not appear to be fully extended in the mixed monolayer, and the data suggest that the terminal TM-GABA group is bent over and possibly less accessible. This could be due to the absence of cohesive interactions between distal end groups in TM-GABA in the mixed films. The consequence is that the GABA is less accessible in the mixed films relative to the pure TM-GABA monolayer. The surface density of GABA groups on an unreduced mixed SAM assembled from a 1:1 TM-GABA:EG6 mixture is $(7.2 \pm 0.06) \times 10^{13}$ GABA cm^{-2}. The adsorbed amount of anti-GABA on the unreduced mixed SAM formed from a 1:1 TM-GABA:EG6 mixture was 3.6×10^{10} antibodies cm^{-2} (Fig. 5B, curve d). The ratio of the adsorbed anti-GABA to the measured GABA in the film is $\sim(3.6 \times 10^{10})/(7.2 \times 10^{13}) = 5 \times 10^{-4}$. This is substantially less than expected based on the density of GABA in the mixed film and on antibody binding to the full TM-GABA film. The lower apparent accessibility of the GABA groups is attributed to the "bent" TM-GABA terminal group. Thus, shorter or different inert materials would need to be explored if there were further requirements for controlling the density of TM-GABA. For the purposes of this study, however, the measurements with the full TM-GABA film both show the bioactivity of this material and provide an upper bound for the percent conversion of TM-GABA following electrochemical reduction.

5. Conclusions

The present investigation demonstrates preparation of a well-defined surface capable of releasing the neurotransmitter GABA upon electrochemical reduction. A new compound TM-GABA (**1**) that is derivatized with an oligo(ethylene glycol) tail and an electroactive quinone group has been synthesized, and was deposited onto gold surfaces through the self-assembly process. Although there is no direct evidence for close packing, the XPS measurements confirmed the formation of an ordered TM-GABA monolayer with a tilt angle of ∼30° relative to the surface normal. The surface coverage is in a range for closely packed monolayers. Upon application of an electrochemical potential of −700 mV, the quinone groups are reduced to hydroquinone, which then rapidly lactonizes with release of GABA. SPR experiments with anti-GABA antibody further confirmed the surface bio-specificity of TM-GABA SAM. Self-assembled monolayer of TM-GABA is resistant to the non-specific interaction with protein. The observed properties of the TM-GABA surface studied here encourage further work to explore the use of controllable biomolecule-releasing surfaces for applications in neuroscience and biomedicine.

Acknowledgments

This work was supported by the University of Illinois Intercampus Research Initiative in Biotechnology (IRIB) program and by grant EY13693 from the National Institutes of Health. C. Yan was supported in part by DOE award number DEFGO2-91ER45439. The XPS facilities used are in the Center for Microanalysis of Materials, University of Illinois at Urbana-Champaign, which is partially supported by the U.S. Department of Energy under Grant DEFG02-91-ER45439. D.R.P. is a Senior Scientific Investigator of Research to Prevent Blindness (New York, NY).

References

[1] W.-S. Yeo, M. Mrksich, Angew. Chem. Int. Ed. 42 (2003) 3121.
[2] R. Blonder, E. Katz, I. Willner, V. Wray, A.F. Bückmann, J. Am. Chem. Soc. 119 (1997) 11747.
[3] W.-S. Yeo, C.D. Hodneland, M. Mrksich, ChemBioChem 2 (2001) 590.
[4] M.N. Yousaf, M. Mrksich, J. Am. Chem. Soc. 121 (1999) 4286.
[5] C.D. Hodneland, M. Mrksich, J. Am. Chem. Soc. 122 (2000) 4235.
[6] U. Saifuddin, T.Q. Vu, M. Rezac, H. Qian, D.R. Pepperberg, T.A. Desai, J. Biomed. Mater. Res. A 66 (2003) 184.
[7] A. Santos, M.S. Humayun, E. de Juan Jr., R.J. Greenberg, M.J. Marsh, I.B. Klock, A.H. Milam, Arch. Ophth. 115 (1997) 511.
[8] N.E. Medeiros, C.A. Curcio, Invest. Ophth. Vis. Sci. 42 (2001) 795.
[9] R.E. Marc, B.W. Jones, C.B. Watt, E. Strettoi, Progr. Retinal Eye Res. 22 (2003) 607.
[10] M.C. Peterman, J. Noolandi, M.S. Blumenkranz, H.A. Fishman, Proc. Natl. Acad. Sci. USA 101 (2004) 9951.
[11] T.Q. Vu, S. Chowdhury, N.J. Muni, H. Qian, R.F. Standaert, D.R. Pepperberg, Biomaterials 26 (2005) 1895.
[12] A.N.K. Lau, L.L. Miller, J. Am. Chem. Soc. 105 (1983) 5271.
[13] B. Zinger, L.L. Miller, J. Am. Chem. Soc. 106 (1984) 6861.
[14] B. Zinger, L.L. Miller, J. Electroanal. Chem. 181 (1984) 153.
[15] R.L. Blankespoor, A.N.K. Lau, J. Org. Chem. 49 (1984) 4441.
[16] R.G. Nuzzo, D.L. Allara, J. Am. Chem. Soc. 105 (1983) 4481.
[17] A.R. Bishop, R.G. Nuzzo, Curr. Opin. Colloid Interface Sci. 1 (1996) 127.
[18] M. Mrksich, G.M. Whitesides, Annu. Rev. Biophys. Biomol. Struct. 25 (1996) 55.
[19] M. Mrksich, G.M. Whitesides, ACS Symp. Ser. Chem. Biol. Appl. Polyethylene Glycol 680 (1997) 361.
[20] L.A. Carpino, S.A. Triolo, R.A. Berglund, J. Org. Chem. 54 (1989) 3303.
[21] B. Wang, S. Liu, R.T. Borchardt, J. Org. Chem. 60 (1995) 539.
[22] A. Zheng, D. Shan, B. Wang, J. Org. Chem. 64 (1999) 156.
[23] D. Muller, I. Zeltser, G. Bitan, C. Gilon, J. Org. Chem. 62 (1997) 411.
[24] C. Bamdad, Biophys. J. 75 (1998) 1997.
[25] K.L. Amsberry, R.T. Borchardt, Pharmacol. Res. 8 (1991) 323.

[26] G. Beamson, D. Briggs, High-Resolution XPS of Organic Polymers, The Scienta ESCA 300 Database, Wiley, Chichester, UK, 1992.
[27] D.A. Shirley, Phys. Rev. B 5 (1972) 4709.
[28] N. Lavrik, D. Leckband, Langmuir 16 (2000) 1842.
[29] L.S. Jung, C.T. Campbell, T.M. Chinowsky, M.N. Mar, S.S. Yee, Langmuir 14 (1998) 5636.
[30] M.G. Nicolaou, J.L. Wolfe, R.L. Schowen, R.T. Borchardt, J. Org. Chem. 61 (1996) 6633, and references therein.
[31] A.J. Bard, I. Rubinstein (Eds.), Electroanalytical Chemistry, vol. 19, Dekker, New York, 1996.
[32] J.P. Folkers, P.E. Laibinis, G.M. Whitesides, Langmuir 8 (1992) 1330.
[33] C. Yan, A. Gölzhäuser, C. Wöll, M. Grunze, Langmuir 15 (1999) 2414.
[34] P. Harder, M. Grunze, R. Dahint, G.M. Whitesides, P.E. Laibinis, J. Phys. Chem. B 102 (1998) 426.
[35] C. Cotton, A. Glidle, J.M. Cooper, Langmuir 14 (1998) 5139.
[36] S. Hofmann, in: D. Briggs, M.P. Seah (Eds.), Practical Surface Analysis, Wiley, Chichester, UK, 1993.
[37] C.D. Bain, G.M. Whitesides, J. Am. Chem. Soc. 111 (1989) 7164.
[38] H. Bruijn, P. Kooyman, J. Greve, Appl. Opt. 31 (1992) 440.
[39] A. Kolomenskii, P. Gerson, H. Schuessler, Appl. Opt. 36 (1997) 6539.
[40] G.L. Kenausis, H. Vörös, D.L. Elbert, N. Huang, R. Hofer, L. Rui-Taylor, M. Textor, J.A. Hubbell, N.D. Spencer, J. Phys. Chem. B 104 (2000) 3298.
[41] B. Zhu, T. Eurell, R. Gunawan, D. Leckband, J. Biomat. Sci. Polym. Ed. 56 (2001) 406.
[42] R. Isreals, F.A.M. Leemakers, G.J. Fleer, Macromolecules 28 (1995) 1626.
[43] S. Milstien, L.A. Cohen, J. Am. Chem. Soc. 94 (1972) 9158.
[44] F. Gao, S.M. Wu, J. Neurophysiol. 80 (1998) 1752.
[45] B. Roska, E. Nemeth, L. Orzo, F.S. Werblin, J. Neurosci. 20 (2000) 1941.
[46] W. Shen, M.M. Slaughter, J. Physiol. 530 (2001) 55.
[47] E.A. Padlan, Mol. Immunol. 31 (1994) 169.